The 9th European Congress on Computational Methods in Applied Sciences and Engineering
ECCOMAS Congress 2024
3 – 7 June 2024, Lisboa, Portugal

FLUID-STRUCTURE INTERACTION SIMULATION OF TRANSCATHETER AORTIC VALVE IMPLANTATION USING SMOOTHED PARTICLE HYDRODYNAMICS

C. CATALANO[1], O. ZAHALKA[2], T. TURGUT[2], V. BOUWMAN[2] AND S. PASTA[1,3]

[1] Department of Engineering, University of Palermo, Viale delle Scienze Ed.8, Palermo, Italy,
chiara.catalano02@unipa.it
[2] 4RealSim Services BV, Groene Dijk 2B, 3401 NJ IJsselstein, Netherlands
[3] Interventional Cardiology Unit, IRCCS ISMETT, Via Tricomi 5, Palermo, Italy,
salvatore.pasta@unipa.it

Key words: Finite element method, smoothed particle hydrodynamics, fluid structure interaction, aortic valve, transcatheter aortic valve implantation.

Summary. This study explores the structural and hemodynamic response in patients who underwent transcatheter aortic valve implantation (TAVI) using a fluid-structure interaction (FSI) approach based on meshless smoothed particle hydrodynamics (SPH). Unlike previous studies that assumed rigid components, this study developed a SPH model capable of accounting for two-way fluid-solid interaction (FSI) for all parts (ie, patient anatomy and device components). The model integrated the Sapien 3 (S3) TAVI device (Edwards Lifesciences, Irvine, CA) into personalized anatomical frameworks and employed rigorous verification and validation activities. Patient-specific pressure and flow boundary conditions were used for simulations. Results from 10 patient-specific simulations showed that the SPH approach realistically simulated the dynamic response of the S3 device during the cardiac cycle, providing insights into device performance, and aortic root deformation. In conclusion, this study presents a comprehensive computational framework for TAVI, leveraging SPH for accurate fluid-solid interaction analysis, which could advance post-TAVI hemodynamic understanding and facilitate the development of an in-silico platform for biomedical device testing.

1 INTRODUCTION

Transcatheter aortic valve implantation (TAVI) has emerged as a pivotal minimally invasive procedure for treating aortic valve diseases, particularly in high-risk patients. It has witnessed remarkable technological advancements, inspiring extensive investigations into structural and hemodynamic response using *in-silico* modelling. Computational models play a crucial role in optimizing TAVI procedures, offering insights into complex fluid-structure interactions and device performance [1].

Numerous studies have employed computational fluid dynamics (CFD) analysis to examine hemodynamics in the post-TAVI configuration [2-5]. CFD simulations require rigid geometries [4, 6, 7], which may inadequately capture the complexities of host-device interaction within the fluid domain. In this context, fluid-structure interaction (FSI) simulations emerge as valuable

alternatives, facilitating the interaction between geometries and the fluid domain, thereby yielding more precise outcomes. Among FSI methodologies, the boundary conforming arbitrary Lagrangian-Eulerian (ALE) method [8, 9] alongside the non-boundary conforming immersed boundary method (IBM) stand out [10, 11]. Though the ALE method can initially yield accurate results at the interface, ALE-related effectiveness and efficiency can diminish over time, especially in simulations involving significant structural deformations, such as those of the heart valve. This is primarily because the ALE method involves remeshing or updating the mesh as the simulation progresses, which increases computational costs and complexity in implementation. On the other hand, while the IBM is powerful for applications involving complex and moving boundaries, it may struggle with accuracy and efficiency in scenarios involving fine-scale interface details or high fluid-structure interaction complexity [12]. With this regard meshfree approaches as the Lattice-Boltzmann (LBM) and smoothed particle hydrodynamics (SPH) results more appealing for complex heart valve simulations. The latter consists of a meshless Lagrangian technique employed for the numerical solution of partial differential equations. Unlike traditional methods SPH utilizes particlea to represent the fluid, with material properties assigned to each point [13].

Despite numerous efforts to simulate cardiovascular problems using the meshless SPH approach, only a few investigations have focused on the aortic valve [4, 5, 7, 14-16]. For instance, Caballero et al. [14] performed a comprehensive computational analysis to investigate the impact of TAVI on mitral regurgitation severity and left heart dynamics in one retrospective clinical case. Pasta et al. [4] proposed a patient-specific computational framework to assess regions at high risk of paravalvular leakage when implanting balloon-expandable and self-expandable transcatheter heart valves (THVs) in bicuspid patients. More recently, Laha and colleagues [16] modeled valve dynamics within a patient-specific anatomy using SPH, suggesting a novel framework to estimate wall shear stress and other relevant hemodynamic parameters.

While these computational investigations have addressed several key challenges in modeling the intricate biomechanical interaction between the heart valve and blood flow, to the best of our knowledge, the present study aims to conduct a series of realistic patient-specific TAVI SPH simulations and validate device performance parameters against clinical data. This advancement marks a notable progress towards precise and tailored FSI simulations with improved reliability. Unlike prior studies [14, 15, 17] that assumed rigid components, we have developed an SPH model that accurately represents the complete FSI within patient-specific anatomy and device.

2 METHODS

2.1 Patient study population

The study comprised a cohort of 10 patients diagnosed with severe aortic valve stenosis, aged between 75 and 91 years, who underwent transcatheter aortic valve implantation (TAVI) employing either the 23-mm or 26-mm SAPIEN 3 (S3) Ultra device (Edwards Lifesciences, Irvine, USA). TAVI procedure was conducted via transfemoral access under general anesthesia, positioning the S3 device with one-third of its length oriented towards the left ventricle. Neither pre-dilation nor over-expansion of the device was undertaken. Ethical approval and informed

consent were secured from all participants at IRCCS ISMETT hospital. Upon in-hospital admission, demographic data and brachial cuff pressure measurements were obtained. Assessment of the stenotic aortic valve's function was conducted via Doppler echocardiography. Furthermore, ECG-gated CT imaging with contrast-agent was performed to compute the aortic valve annulus dimensions, facilitating pre-planning for the optimal device size. This enabled the acquisition of two distinct sets of CT images depicting systolic and diastolic phases prior to the TAVI procedure. Post-TAVI CT imaging was conducted as part of the study protocol. However, due to renal dysfunction associated with advanced age, a follow-up CT scan during the short-term post-procedural period was deemed unfeasible for some patients.

2.2 Finite element modeling of TAVI

The patient-specific domain and the balloon expandable S3 Ultra device were developed in accordance with the methodology adopted by our research group, as detailed in prior publications [18, 19]. Specifically, pre-TAVI CT images captured at the diastolic phase were processed in Mimics software (Materialise, Leuven, Belgium) to segment the anatomy of the aortic root and calcifications through semi-automatic thresholding techniques [20]. Given the limited visibility of native leaflet anatomies on the CT scans, a parametric modeling approach based on anatomical measurements was adopted for the development of the aortic valve model [21].

The S3 stent frame was meshed with surface elements (SFM3D4R) tied with beam elements (B31). This simplification is justified as the parameter of interest is the radial stiffness rather than the stress-strain rate in the cross-section, with a neglecting difference among stent expanded diameter between surface and solid model of less than 1%. Inner and outer skirt were meshed with surface element as well as the leaflet, which were developed through a forming simulation technique [22].

The isotropic hyperelastic Ogden material model was used to characterize the mechanical properties of the native aortic leaflets. The aorta followed a linear elastic material behavior, while calcifications were characterized by an elastoplastic model. The cobalt-chromium material behavior characterizing the stent frame was modeled using a combination of isotropic elasticity and Johnson-Cook plasticity to account for hardening and rate material dependence. Details on the adopted material parameters can be found on [19, 23].

The TAVI procedure was simulated utilizing the Abaqus/Explicit solver, enabling a dynamic non-linear problem in the range of large deformation and complex contact interactions as done previously [19]. Structural simulations included device crimping, recoil, and deployment of the S3 within the aortic annulus with an implantation depth determined from post-TAVI angio-CT imaging. Contact conditions were established for the surface skin of the S3. To mitigate the risk of unintended penetration during device assembly, a procedural step was implemented to displace calcifications and native valve leaflets using a cylindrical surface. This displacement was conducted while maintaining the implanted device's shape through the imposition of zero-velocity boundary conditions on the stent frame.

Model credibility was established in accordance with ASME V&V40 standards by conducting numerical verification activities on the TAVI model at level component, as detailed in a prior publication. This entailed the rigorous assessment of different modeling techniques

and element mesh types, as well as the influence of various solver parameters, on the model's response [24].

2.3 SPH-Based Fluid-Solid Interaction Analysis

SPH is a fully Lagrangian modeling scheme that discretizes continuum equations by interpolating particle properties within the solution domain using a kernel function W using the properties of its neighboring particles. This method involves the properties of neighboring particles to compute values at a given point. Mathematically, for a particle b with a physical property A_b, the interpolated value at position r is given by [25]:

$$A_S(r) = \sum_b m_b \frac{A_b}{\rho_b} W(r - r_b, h) \quad (1)$$

Here, A_b denotes any physical property of particle b within the neighboring domain, which is limited by the influence length h of the kernel, relative to particle a at position r.

In this study, the default cubic kernel formulation was adopted. By employing this cubic spline kernel function and its derivatives, the governing equations of fluid flow—namely, the conservation of mass, momentum, and energy—can be recast in the SPH framework. This allows for the equations to be discretized and solved in a Lagrangian context, leveraging the properties and positions of particles within the influence domain defined by the kernel function.

SPH analysis was implemented in Abaqus, starting with the deformed anatomy of the patient model featuring the deployed S3 Ultra device. Additionally, two fluid reservoirs were strategically attached to each end of the aorta using tie constraints. The geometries of the reservoirs were designed in the CAD software Rhinoceros (v.5.5, McNeel & associates, SP), utilizing the plugin Grasshopper to create a parametric model that configures the reservoir shape and attachment to each patient's anatomy. Both reservoirs are modeled with surface elements lacking assigned stiffness, allowing their volumes to fluctuate during cardiac simulations.

Once the reservoir geometries were defined, the fluid domain was defined by generating the SPH particles by converting the solid domain in discrete particle elements. The SPH particles were created through background grid conversion in a data-check job. The solid model through which particles are generated and the full patient-specific TAVI SPH model are showed in Figure 1.

The fluid domain was modeled according to the linear Hugoniot equation of state. Blood is assumed incompressible and Newtonian. Particle discretization and material properties are summarized in Table 1.

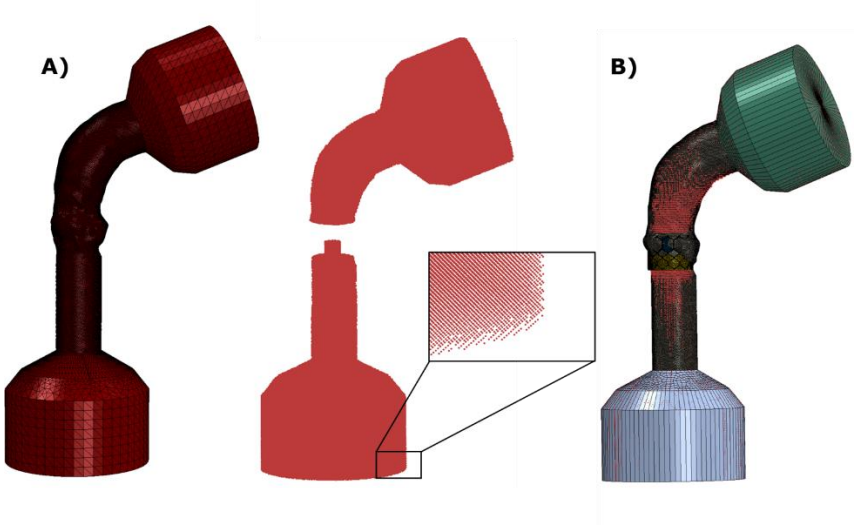

Figure 1: A) Finite element solid mesh and particle distribution; B) Patient-specific TAVI SPH full model

Table 1: Particle discretization and material properties of the fluid domain

Particle diameter	0.9 mm
Density, ρ	1.0E-09 tonne/mm^3
Wave speed, c_0	7.5E+04 mm/s
Grüneisen ratio, Γ_0	0
Hugoniot curve slope, s	0
Viscosity, η	3.0E-09 Mpa*s
Bulk viscosity damping coefficient	0.006

Interactions between the fluid particles and the patient-specific TAVI model were defined as contact pairs within the general contact definition, enabling the interaction between solid parts and particles and ensuring a realistic simulation of post-TAVI hemodynamics.

Physiological pressures and flow waveforms as derived from clinical data were adopted for simulations. Patient heart rate, cuff pressure and echocardiography data were the starting point to scale the duration and offset of boundary conditions within the TAVI SPH model [26]. Figure 2 displays pressure and flow rate waveforms tailored for a representative patient.

During the systolic phase, the flow is governed by the flow rate curve, which is converted to a velocity boundary condition on the LV reservoir. This determine blood particle motion towards the deployed device by mimicking LV chamber contraction. During the diastolic phase, the velocity boundary condition is deactivated, and LV and aortic pressures control the flow due to the pressure difference to favor the development of a reverse flow and valve leaflet

closure. The aortic reservoir behaves as a fluid collector during systole and contracts during diastole to simulate in-vivo arterial compliance. Switching the flow boundary condition on and off is achieved by using a single truss element with temperature-dependent stiffness properties.

The vessel is initialized with a load condition derived from the structural TAVI simulation, which is then imported into the SPH model using a predefined field. Specifically, at the start of the fluid simulations, the device leaflets are in a stress-free state, while the elastic recoil of the aortic root and calcified valve leaflets is balanced by the radial force exerted by the expanded device frame.

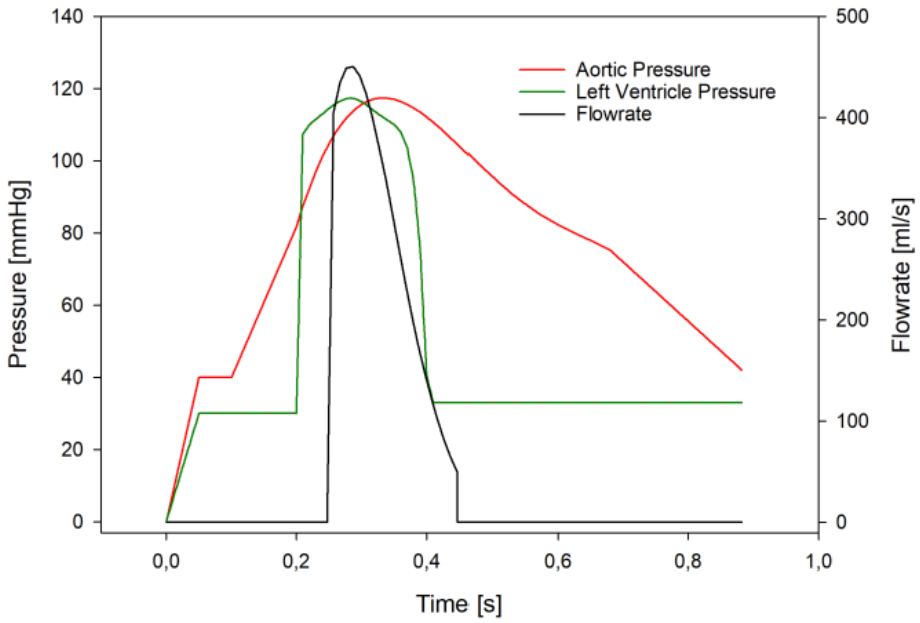

Figure 2: Physiological pressure and flow waveforms derived from patient-specific clinical data

By exploiting the flow pressure and velocity curves obtained from the simulation, main quantities assessing valve performance can be computed according to ISO 5840-1 standard [27]. Specifically, outputs of interest were effective orifice area (EOA), mean and peak pressure gradient (PG).

3 RESULTS

Flow velocities at different phases of the cardiac cycle are shown in Figure 3 for a representative patient-specific TAVI SPH model. Notably, a strong flow jet is developed at systole phase from the opened device valve leaflets, while during diastole an efficient sealing of the leaflets is accomplished, preventing reverse flow.

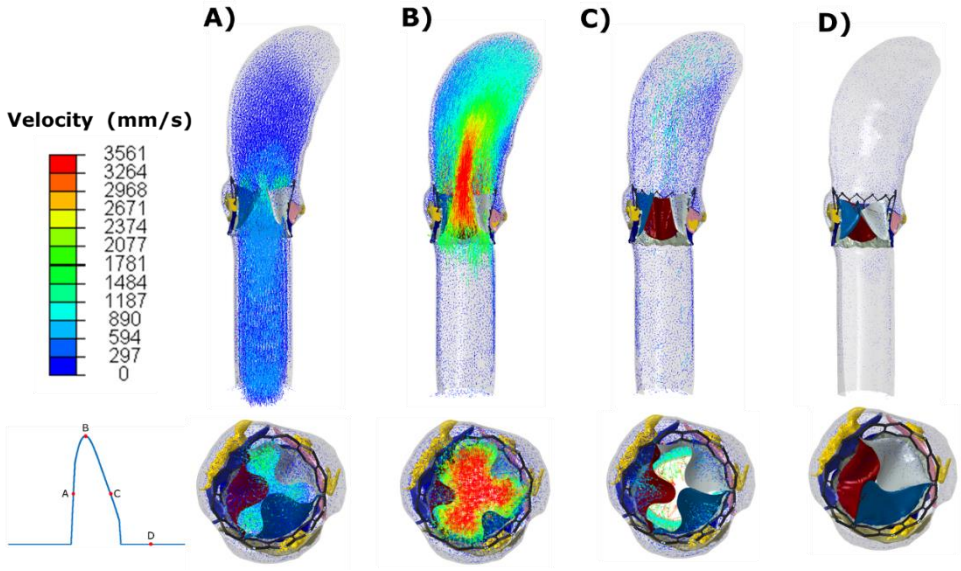

Figure 3: Flow velocities for a representative patient case at A) acceleration, B) systole, C) deceleration and D) diastole phases.

For n.10 patient-specific SPH simulations, the peak velocity was 2.45±0.47 m/s with respect to the echocardiography evaluation of 2.5±0.41 m/s, the SPH-related EOA was 1.53±0.47 cm^2 with respect to the echocardiographic evaluation of 1.41±0.15 cm^2, the SPH-related mean PG was 18.83±5.64 mmHg versus the clinical estimation of mean PG 13.67±4.55 mmHg, while the peak PG was 31.50±10.95 mmHg against the clinical estimation of peak PG 27.72±7.41 mmHg.

A good level of agreement was quantitatively found between patient-specific simulation results and correspondent post-procedural clinical data, with certain variables showing more accordance with the clinical data. Overall relative error between clinical data and simulation outputs were in the range of 1.7% - 24.2%, with the PG estimations showing the highest differences between in-silico model and reality.

To further compare simulation outputs and correspondent patient-specific clinical quantities, the cumulative density function has been plotted for both simulations and clinical data (figure 4), and the area metric was employed as a quantitative measure of the discrepancy between predictions and data. The computed area metric between predictions and real patient data were 12.8% for the jet velocity (m/s), 5.67% for the EOA (cm^2), 7.94% for the peak PG (mmHg) and 18.61% for the mean PG.

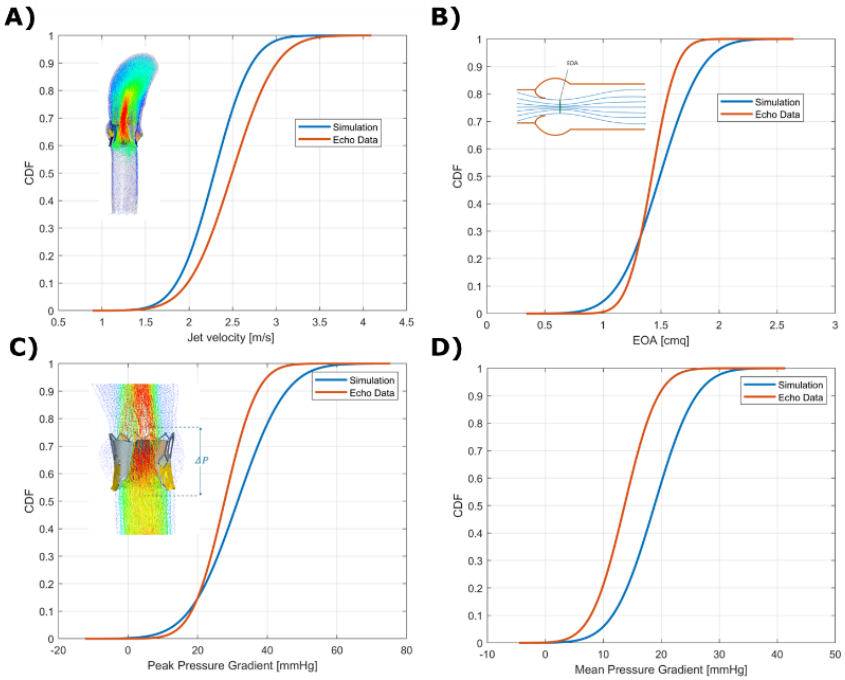

Figure 4: CDF of simulation and clinical data plotted for A) jet velocity, B) EOA, C) peak PG and D) mean PG

4 DISCUSSIONS

A novel computational framework enabling FSI analysis of patient-specific TAVI using SPH has been proposed. This framework simulates the fluid dynamics of the deployed S3 device, allowing for an investigation of the device's hemodynamic performance throughout an entire heartbeat for each analyzed patient. Validation of device performance parameters against clinical echocardiographic post-TAVI data improves the credibility of the proposed SPH technique.

Although a few studies in the literature have investigated the hemodynamic implications of TAVI [8-11], most have assumed a rigid aortic wall, used a simplified THV model, or did not account for patient-specific anatomy or boundary conditions. These limitations restrict the FSI capability in assessing cardiovascular problems accurately.

This study presented the result of n.10 patient-specific SPH simulations tailored to real patients, incorporating a highly accurate structural TAVI model and SPH-related flow simulations accounting for the TAVI deployment and vessel configuration. This model enables full coupling between anatomic components, the device, and blood fluid flow. Consequently, the proposed approach does not only accurately mimic the real procedure, but also enhances the model credibility by proposing a validation comparing the cumulative distribution function and determining the difference among clinical and computational profiles (ie, the area metric).

To achieve this goal, we leverage of the same solver for simulating the S3 device deployment and then the FSI given the dynamic phenomenon and contact problems. Moreover, the TAV model in this study completely matches the design of the Edwards Sapien valve clinically implanted in patients. This alignment ensures the clinical relevance of the simulations.

Our study also pioneers the modeling of a flexible valve within patient-specific aortic vasculature using SPH. We adopted tailored boundary conditions to each patients accounting for clinical cuff pressure data collected during in-hospital admission.. This approach ensures that simulation outcomes accurately reflect the specific patient's cardiovascular conditions, enhancing the model's predictive capabilities for TAVI procedures.

To further enhance clinical relevance, this study successfully validated simulation results against patient-specific clinical data, with relative errors between predictions and clinical data ranging from 1.7% to 24.2%. Detailed comparisons were made by plotting the cumulative distribution function of relevant S3-related outputs, such as EOA, PG, and peak velocity, and quantifying the level of agreement using area metric computation. Peak velocity and EOA showed better agreement between real patient-specific values derived from echocardiography data and predicted values, with area metrics of 12.8% and 5.67%, respectively. Conversely, peak and mean PG showed less agreement between predictions and clinical data, with area metrics of 7.94% and 18.61%, respectively. Discrepancies could be caused by the qualitative assessment of echocardiography, instrumentation accuracy as well as intra and inter-operator variability.

Overall, the findings demonstrate the computational framework capability to realistically simulate the dynamic response of the S3 device within the patient's anatomy during the cardiac cycle. This provides valuable insights into efficient sealing, device opening and closing dynamics, and aortic root deformation [25].

However, the study acknowledges limitations such as potential variability in echocardiographic measurements and the need for further verification of the SPH model to enhance its credibility. Future work will focus on addressing these limitations and refining the model to ensure even greater accuracy and reliability.

Our study extends the applicability of SPH by presenting a comprehensive computational framework for TAVI. By leveraging SPH for accurate FSI analysis and providing in-silico techniques for modeling post-TAVI FSI, this study improved our understanding of the structural and hemodynamic performance of TAVI patients.

5 CONCLUSIONS

A fully coupled FSI approach combining SPH with nonlinear FE models for simulating TAVI procedure was implemented in this study. By incorporating a realistic TAVI, this SPH approach addresses limitations in previous studies, such as the assumption of a rigid aortic wall, simplified THV models, not-fully coupled FSI approach and a lack of patient-specific anatomy and boundary conditions. The proposed methodology advances the understanding of post-TAVI hemodynamic and holds promise for the development of an in-silico platform for biomedical device testing.

ACKNOWLEDGMENT

This project has received funding from the European Union’s Horizon 2020 research and innovation programme under grant agreement No 101017523.

REFERENCES

1. Catalano, C. and S. Pasta, *On the Modeling of Transcatheter Therapies for the Aortic and Mitral Valves: A Review.* Prosthesis, 2022. **4(1)**: p. 102 - 112.
2. Luraghi, G., et al., *On the Modeling of Patient-Specific Transcatheter Aortic Valve Replacement: A Fluid-Structure Interaction Approach.* Cardiovasc Eng Technol, 2019. **10**(3): p. 437-455.
3. Ghosh, R.P., et al., *Numerical evaluation of transcatheter aortic valve performance during heart beating and its post-deployment fluid-structure interaction analysis.* Biomech Model Mechanobiol, 2020. **19**(5): p. 1725-1740.
4. Pasta, S. and C. Gandolfo, *Computational Analysis of Self-Expanding and Balloon-Expandable Transcatheter Heart Valves.* Biomechanics, 2021. **1**(1): p. 43-52.
5. Pasta, S., et al., *Transcatheter heart valve implantation in bicuspid patients with self-expanding device.* Bioengineering, 2021. **8**(7): p. 91.
6. Caballero, A., et al., *The impact of balloon-expandable transcatheter aortic valve replacement on concomitant mitral regurgitation: a comprehensive computational analysis.* Journal of the Royal Society Interface, 2019. **16**(157): p. 20190355.
7. Mao, W., K. Li, and W. Sun, *Fluid-Structure Interaction Study of Transcatheter Aortic Valve Dynamics Using Smoothed Particle Hydrodynamics.* Cardiovasc Eng Technol, 2016. **7**(4): p. 374-388.
8. Ghosh, R.P., et al., *Comparative Fluid–Structure Interaction Analysis of Polymeric Transcatheter and Surgical Aortic Valves' Hemodynamics and Structural Mechanics.* Journal of biomechanical engineering, 2018. **140**(12): p. 121002.
9. Basri, A.A., et al., *Fluid structure interaction on paravalvular leakage of transcatheter aortic valve implantation related to aortic stenosis: a patient-specific case.* Computational and mathematical methods in medicine, 2020. **2020**.
10. Borazjani, I., *Fluid–structure interaction, immersed boundary-finite element method simulations of bio-prosthetic heart valves.* Computer Methods in Applied Mechanics and Engineering, 2013. **257**: p. 103-116.
11. Flamini, V., A. DeAnda, and B.E. Griffith, *Immersed boundary-finite element model of fluid–structure interaction in the aortic root.* Theoretical and computational fluid dynamics, 2016. **30**: p. 139-164.
12. Bavo, A.M., et al., *Fluid-structure interaction simulation of prosthetic aortic valves: comparison between immersed boundary and arbitrary Lagrangian-Eulerian techniques for the mesh representation.* PloS one, 2016. **11**(4): p. e0154517.
13. Lluch, È., et al., *Breaking the state of the heart: meshless model for cardiac mechanics.* Biomechanics and modeling in mechanobiology, 2019. **18**: p. 1549-1561.
14. Caballero, A., et al., *Modeling Left Ventricular Blood Flow Using Smoothed Particle Hydrodynamics.* Cardiovasc Eng Technol, 2017. **8**(4): p. 465-479.
15. Scuoppo, R., et al., *Parametric analysis of transcatheter aortic valve replacement in transcatheter aortic valve replacement: evaluation of coronary flow obstruction.* Front Bioeng Biotechnol, 2023. **11**: p. 1267986.
16. Laha, S., et al., *Smoothed particle hydrodynamics based FSI simulation of the native and mechanical heart valves in a patient-specific aortic model.* Scientific Reports, 2024. **14**(1): p. 6762.
17. Mao, W., et al., *Fully-coupled fluid-structure interaction simulation of the aortic and mitral valves in a realistic 3D left ventricle model.* PLoS One, 2017. **12**(9): p. e0184729.
18. Catalano, C., et al., *3D Printing and Computational Modeling for the Evaluation of LVOT obstruction in Transcatheter Mitral Valve Replacement.* V Cirp Conference on Biomanufacturing, 2022. **110**: p. 273-278.
19. Catalano, C., et al., *On the Material Constitutive Behavior of the Aortic Root in Patients with Transcatheter Aortic Valve Implantation.* Cardiovascular Engineering and Technology, 2024. **15**(1): p. 95-109.
20. Rinaudo, A., et al., *Biomechanical implications of excessive endograft protrusion into the aortic arch after thoracic endovascular repair.* Computers in Biology and Medicine, 2015. **66**: p. 235-241.
21. Pasta, S., et al., *Three-dimensional parametric modeling of bicuspid aortopathy and comparison with computational flow predictions.* Artif Organs, 2017. **41**(9): p. E92-E102.

22. Bailey, J., N. Curzen, and N.W. Bressloff, *Assessing the impact of including leaflets in the simulation of TAVI deployment into a patient-specific aortic root.* Comput Methods Biomech Biomed Engin, 2016. **19**(7): p. 733-44.
23. Catalano, C., et al. *An Inverse Analysis for the Assessment of Material Properties of TAVI Patients*. in *Eighth National Congress of Bioengineering–Proceedings 2023*. 2023. Patron Editore Srl.
24. Catalano, C., et al., *Establishing In-silico Credibility of Patient-Specific Finite-Element Model in a Virtual Cohort*, in *Lecture Notes in Computational Vision and Biomechanics*. 2024. p. 311-318.
25. Monaghan, J.J., *Smoothed particle hydrodynamics.* In: Annual review of astronomy and astrophysics. Vol. 30 (A93-25826 09-90), p. 543-574., 1992. **30**: p. 543-574.
26. Pasta, S., et al., *Numerical simulation of transcatheter mitral valve replacement: The dynamic implication of LVOT obstruction in the valve-in-ring case.* Journal of Biomechanics, 2022. **144**.
27. ISO 5840-1:2021, *Cardiovascular implants—Cardiac valve prostheses—Part 1: General requirements.* International Organization for Standardization, 2021, Geneva, Switzerland.